IEEE Access
Multidisciplinary | Rapid Review | Open Access Journal

IEEE POWER & ENERGY SOCIETY SECTION

Received November 24, 2021, accepted December 20, 2021, date of publication December 24, 2021,
date of current version January 20, 2022.

Digital Object Identifier 10.1109/ACCESS.2021.3138549

Monte-Carlo Evaluation of Residential Energy System Morphologies Applying Device Agnostic Energy Management

STEFAN ARENS, SUNKE SCHLÜTERS, BENEDIKT HANKE, KARSTEN VON MAYDELL, AND CARSTEN AGERT
DLR Institute of Networked Energy Systems, 26129 Oldenburg, Germany
Corresponding author: Stefan Arens (stefan.arens@dlr.de)

ABSTRACT Decarbonization requires new energy systems components to mitigate fossil fuel dependency, for instance electric vehicles and heat pumps, forming a sector integrated energy system. Energy management is a promising approach to integrate these devices more efficiently by orchestrating the respective consumption and generation. This study investigates the advantage of an advanced energy management algorithm that is applied to varying energy system scenarios. The energy management algorithm is based on economic principles and the system topology is represented by a rooted tree. Grid elements form parents, which act as auctioneers and devices act according to type specific demand and supply functions. This algorithm is compared to an approach where devices are not coordinated, at a system scale of six households. In order to account for different characteristics of the energy system, the different scenarios are defined according to a morphological analysis and are analysed by means of Monte-Carlo simulation. These scenarios vary the PV generation, heating technology, and building insulation. It is shown that the algorithm reduces peak loads across all scenarios by around 15 kW. Other key performance indicators, such as own consumption and self-sufficiency show a dependency on the scenarios, although the algorithm outperforms the reference in each one, achieving an increase in own consumption of at least 13 p.p. and 22 p.p. in terms of self-sufficiency.

INDEX TERMS Energy management, Monte-Carlo methods, scenario analysis, systems modelling.

I. LIST OF ABBREVIATIONS

PV	Photovoltaic.
CHP	Combined Heat and Power.
BEV	Battery Electric Vehicle.
HES	Home Energy Storage.
BAK	Backup.
DHW	Domestic Hot Water.
SH	Space Heating.
TS	Time Series.
PLR	Part Load Ratio.
HP	Heat Pump.
COP	Coefficient of Power.
LPG	Load Profile Generator.
HDD	Heating Degree Day.
DSS	Degree of Self-Sufficiency.

The associate editor coordinating the review of this manuscript and approving it for publication was Shafi K. Khadem.

II. INTRODUCTION

Electricity generation based on renewables such as wind and solar contributes to decarbonize the energy system by replacing fossil fuels [1]–[3]. To further push decarbonization, sector integrated energy systems are developed that enable electricity usage for mobility and heating [4], [5]. Integrating the heat and electricity sector is especially interesting because it also provides flexibility due to heat storages and variable power operation of the heat generating devices [6]. Heat pump (HP) systems provide energy for heating by using electricity and low temperature environmental heat. They enable the utilization of local energy, provided by PV systems [7], [8]. Micro-CHP systems are another promising technology. These systems co-generate heat and electricity efficiently by the utilisation of waste heat [9]. A CHP system can be based on fuel cells that use hydrogen [10]. Another field of application for hydrogen fuel cells is individual mobility. For mobility application as well as for fuel cells, production of hydrogen should be as less carbon

intensive as possible in order to decarbonate the energy system [11]–[13].

An alternative to fuel cells are battery electric vehicles (BEV) that directly use electricity to provide mobility. Fuel cell based vehicles offer bigger driving ranges [14], whereas BEVs exhibit higher energy efficiencies [15]. Furthermore, the transformation of the energy system adds loads and generators especially in the low voltage grid, imposing new challenges. For example, adding BEVs increase the voltage drop [16] and additional PV systems can cause voltage band violations [17].

The transformation of the energy system is an ongoing process with different possible paths that are usually described by complex scenario modelling. Resulting paths feature vastly different outcomes either due to endogenic factors such as modelling approach or due to exogenic factors that comprise assumed policies and parameters [18]. For example, the split of generation technologies can vary, depending on the model [1]. Furthermore, scenario analyses usually have low spatial resolution, for example countries or even continents, which can not fully represent disaggregated effects that are caused on a high spatial resolution [1], [19]. Therefore, the effect caused by different technologies on the high spatial resolution requires further investigation.

Energy management algorithms are developed in order to optimally utilize existing infrastructure and system components. These algorithms orchestrate an energy system and optimize its operation with respect to one or more key performance indicators, such as cost, CO_2 emissions, self-sufficiency, own consumption, grid utilization, or peak load. Constraints express technical limitations due to storage capacity, power limitations, or others. The algorithms are based on a broad range of principles, ranging from linear optimization [20], mixed integer linear optimisation [21], auction mechanisms [22], [23], machine learning [24], game theory [25], [26] and meta heuristics [27]. However, all these algorithms are usually tested within limited scope, using case studies. For example, in [28] the test case consist, among generation and storage nodes, of four loads. Such case studies barely cover the overall real word complexity because load time series vary heavily due to individual behaviour and components [29], [30]. For a household, the implemented technologies are dimensioned according to the specific load requirements, e.g. persons of a household. A simple case study hardly covers the complexity of the real world and a more comprehensive investigation can provide additional insight into the capabilities of an algorithm. Therefore, a systematic algorithm evaluation is proposed.

To evaluate the effect of energy management within a broad scenario space, this study proposes Monte-Carlo simulation. In Mote-Carlo simulation, input parameters are considered uncertain. Distributions are defined for these parameters, which then yield output variables through a model. These output variables form an empirical distribution from which statistical variables are derived to describe the entire system. This methodology can be applied to investigate complex systems where an analytical solution is not possible [31], [32].

In literature, Monte-Carlo simulation is employed to test renewable generation and load scenarios [33]. However, that study does not consider sector integrating technologies. Further application is the uncertainty evaluation of a BEV for a sector integrated energy system [34], [35] and throughput analysis of wireless networks that steer energy systems [36]. A Monte-Carlo approach enables the dynamic dimensioning of energy system components, considering uncertainty from PV generation [37]. Additionally, multiple uncertain parameters can be investigated, for example load, generation, and market price [25].

This study contributes to the evaluation of expected grid requirements in the future and, thus, enhances grid planning capabilities by applying Monte-Carlo simulation. In particular, it systematically determines the advantage of an energy management algorithm by comparing it to a reference. A broad range of energy systems with a high special resolution is studied, based on different scenarios. The small-scale system heterogeneity is addressed by stochastically varying parameters.

This study is structured as follows: Section III describes the algorithm that is based on previous work of the authors [38]. Section IV describes how the different scenarios are implemented, Section V shows the modelling approach to individualize the system components in terms of time series and parameters, Section VI describes the simulation set-up, Section VII shows the results, and Section VIII discusses the results and draws the conclusions.

III. AUCTION-BASED ENERGY MANAGEMENT

This section describes the algorithm, which is used for energy management, according to [38]. Furthermore, the HP and CHP technologies are integrated and the respective parameterizations are described.

A. ALGORITHM DESCRIPTION

The energy management algorithm is based on the continuous Japanese auction. In this auction, an auctioneer states a price and each interested buyer replies with the quantity it is willing to buy at the respective price. The auctioneer increases the price until demand matches supply.

This basic auction mechanism is altered in three ways for energy management application. First, descending the price during an auction is allowed to integrate generation units. Second, price limits are introduced to ensure the termination of the auction. Third, the starting price is set dynamically, depending on the outcome of the previous auction.

The components of the energy system are organized in a rooted tree. The leaves of the tree represent electricity consuming or producing devices. The parents represent a component of the underlying electricity grid. Each parent has defined actions during an auction, e.g. achieving a residual power of 0 W. For each auction, a parent states an initial price and the children reply with a quantity of power according to

that price. Therefore, the summed quantity can be evaluated for each parent in the tree. A parent can change the price to alter the quantity of power received and the component are required to update their power response. Note that all leaves must follow the law of supply and demand, thus the general effect of changing the price is known to a parent. The auction terminates if the goal of an auctioneer is fulfilled or no further improvement is possible.

For the rest if this study, the price is called *steering signal* to emphasize its role, which is to the behaviour of the single components in interest of the energy system demands and targets.

B. ADDED TECHNOLOGIES

To investigate a broader scenario space, demand and supply functions for a CHP system, equipped with a backup-heater (BAK), and a HP system are implemented. These functions model the reaction of the respective component according to the steering signal, i.e. determining the power. In its core, they are based on heuristics and can be adopted to individual preferences as they only have to follow the law of supply and demand with respect to the steering signal.

For this study, we only consider CHP systems with a hot water storage and a BAK. The storage reduces the peak thermal power demand of the generation unit by buffering thermal energy. The CHP-units simultaneously generate electricity and heat. Therefore, the steering signal and the storage temperature are the most important parameters for the CHPs demand/supply function. If the storage temperature is low, the heat demand is high and if the steering signal is low, the electrical power generated is low. In addition, two plateaus are added that shift the generation towards higher steering signals and adapt to different storage temperature situations. One prevents the CHP unit from running at high or maximum temperature and the other one ensures thermal generation at minimum storage temperature. In-between these two regions, a transition region, based on the cosine function that enables smooth and flexible power adaptation, is located. The demand and supply function relies on the heat storages minimum and maximum temperature $\theta_{\min}^{\text{storage}}$ and $\theta_{\max}^{\text{storage}}$, the steering signals minimum and maximum value $\text{pr}_{\min}$ and $\text{pr}_{\max}$, the CHP systems maximum electrical power $P_{\max}^{CHP}$. Equation 1 - 2 describe the demand and supply function of a CHP unit and Equation 3 - 4 the BAK one.

$$\begin{aligned}&\text{pr}_{\text{dec}}(\theta, \text{pr})\\ &= \text{pr} + \frac{\theta_{\max}^{\text{storage}} + \theta_{\min}^{\text{storage}} - 2\theta}{\theta_{\max}^{\text{storage}} - \theta_{\min}^{\text{storage}}} \cdot \left(\text{pr}_{\max} - \text{pr}_{\min}\right)\end{aligned} \tag{1}$$

$$\begin{aligned}&P^{CHP}(\theta, \text{pr})\\ &= \begin{cases} P_{\max}^{CHP} & \text{if } \text{pr}_{\text{dec}}(\theta, \text{pr}) \geq \text{pr}_{\max},\\ 0 & \text{if } \text{pr}_{\text{dec}}(\theta, \text{pr}) \leq \text{pr}_{\min},\\ P_{\max}^{CHP} \cdot \cos\left(\frac{\pi}{2} \cdot f_{\text{pr}}(\theta, \text{pr})\right) & \text{otherwise,}\end{cases}\end{aligned} \tag{2}$$

where $f_{\text{pr}}(\theta, \text{pr}) = \frac{1 - \text{pr}_{\text{dec}}(\theta, \text{pr}) + \text{pr}_{\min}}{\text{pr}_{\max} - \text{pr}_{\min}}$.

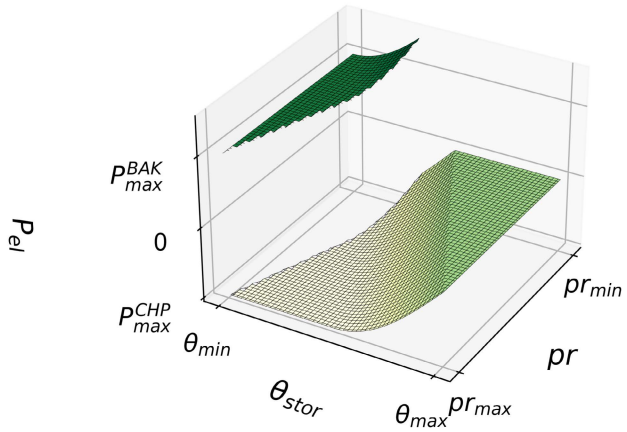

FIGURE 1. Electricity generation of the CHP-BAK system.

The BAK heating system is modelled binary, therefore it can be either on, consuming a power of $P_{\max}^{BAK}$, or off. The activation is modelled with the decision function $\text{pr}_{\text{dec}}^{BAK}(\theta)$ that is based on a threshold temperature, lying above the minimum storage temperature according to $\Delta\theta^{BAK}$. Additionally, a dependency on the steering signal is implemented in the demand function $P^{\text{BAK}}(\theta, \text{pr})$. Note that the BAK system consumes electricity, whereas the CHP-unit produces electricity.

$$\begin{aligned}&\text{pr}_{\text{dec}}^{BAK}(\theta)\\ &= \frac{\text{pr}_{\max} - \text{pr}_{\min}}{\Delta\theta^{BAK}} \cdot \left(\theta_{\min}^{\text{storage}} - \theta\right) + \text{pr}_{\max}\end{aligned} \tag{3}$$

$$\begin{aligned}&P^{\text{BAK}}(\theta, \text{pr})\\ &= \begin{cases} P_{\max}^{BAK} & \text{if } \text{pr} \leq \text{pr}_{\text{dec}}^{BAK}(\theta) \wedge \theta < \theta_{\min}^{\text{storage}} + \Delta\theta^{BAK}\\ 0 & \text{otherwise.}\end{cases}\end{aligned} \tag{4}$$

This electricity and heat co-dependency follows [39] as:

$$\frac{P_{\text{th}}^{CHP}(\theta, \text{pr})}{P^{CHP}(\theta, \text{pr})} = \begin{cases} \text{pc(PLR)} & \text{if PLR} \geq 0.05\\ 0.68 & \text{otherwise,}\end{cases} \tag{5}$$

where $\text{pc(PLR)} = 1.078 \cdot \text{PLR}^4 - 1.974 \cdot \text{PLR}^3 + 1.500 \cdot \text{PLR}^2 - 0.282 \cdot \text{PLR} + 0.6838$ and $\text{PLR} = \frac{P^{CHP}(\theta, \text{pr})}{P_{\max}^{CHP}}$.

The electricity to heat conversion efficiency of the BAK system is assumed as 1.

Figure 1 shows the electricity generation of the combined CPH and BAK system in dependency of the steering signal and the storage temperature and Figure 2 shows the respective heat generation.

The HP demand function consists of two regions. One region spans the low storage temperatures and stimulates heating with high power. The other region spans the high storage temperatures at which the HP consumes less or no power. Both regions emphasize power consumption at low steering signals. However, a plateau and a valley are added to reduce frequent power variations. Equation 6 - 9 describe the

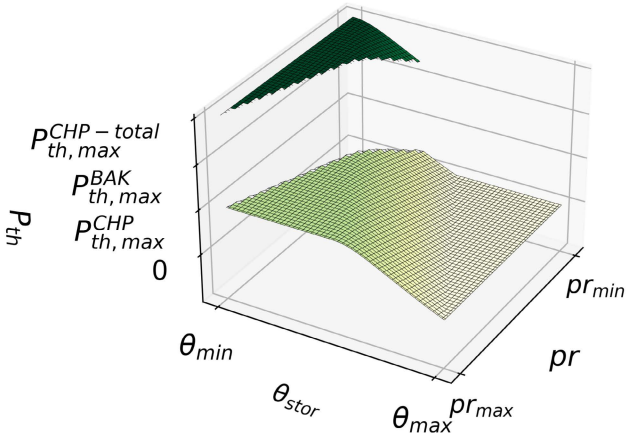

FIGURE 2. Heat generation of the CHP-BAK system.

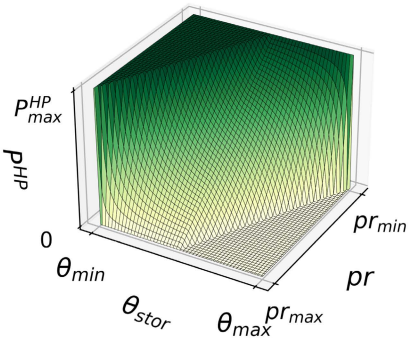

FIGURE 3. Demand function of heat pumps.

demand function in detail and Figure 3 shows the respective function.

The parameter $f_{\text{lim}}(\theta) = \frac{\theta_{\text{min}}^{\text{storage}} + \theta_{\text{max}}^{\text{storage}} - 2\theta}{\theta_{\text{max}}^{\text{storage}} - \theta_{\text{min}}^{\text{storage}}}$ divides the high and low power regions.

If $f_{\text{lim}}(\theta) \geq 0$:

$$d_{\text{dec}}(\theta) = \text{pr}_{\text{min}} + f_{\text{lim}}(\theta) \cdot \text{pr}_{\text{max}} - \text{pr}_{\text{min}} \tag{6}$$

$$P^{HP}(\theta, \text{pr}) = \begin{cases} P^{HP}_{\text{max}} & \text{if pr} \leq d_{\text{dec}}(\theta) \\ \frac{P^{HP}_{\text{max}}}{\text{pr}_{\text{max}} - \text{pr}_{\text{min}}} \cdot (\text{pr} - d_{\text{dec}}(\theta)) + P^{HP}_{\text{max}} & \text{otherwise} \end{cases} \tag{7}$$

If $f_{\text{lim}}(\theta) < 0$:

$$d_{\text{dec}}(\theta) = \text{pr}_{\text{max}} + f_{\text{lim}}(\theta) \cdot \text{pr}_{\text{max}} - \text{pr}_{\text{min}} \tag{8}$$

$$P^{HP}(\theta, \text{pr}) = \begin{cases} 0 & \text{if pr} \leq d_{\text{dec}}(\theta) \\ \frac{P^{HP}_{\text{max}}}{\text{pr}_{\text{max}} - \text{pr}_{\text{min}}} \cdot (\text{pr} - d_{\text{dec}}(\theta)) & \text{otherwise} \end{cases} \tag{9}$$

The conversion from electricity to heat is modelled assuming a constant COP.

An inertia is applied to the heat pump and the CHP unit. This inertia only allows the power to be changed by 10 % of the nominal power per interval. Furthermore, a hysteresis is implemented to prevent successive on and off switching. For example, frequent on and off switching can otherwise occur during summer times when high PV-power is available, the heat storage is almost fully charged, and the heat demand is low. The heat losses would reduce the storage temperature slightly below its maximum temperature. The high PV-power can result in a low steering signal that triggers a HP to run for a short time until the maximum temperature is reached. This procedure would be repeated often which is an undesired operation mode.

IV. MONTE-CARLO SIMULATION

This section describes randomized parameters for the Monte-Carlo simulation. The parameters are divided into scenario dependent and scenario independent parameters. Scenario dependent parameters affect the probability of certain devices being present, thus defining the scenario space. Scenario independent parameters describe general energy system variations.

A. SCENARIO SPACE

From the morphological analysis performed authors of this study in [40], three factors are taken: PV-generation capacity, heating technology, and building insulation, to define different energy system morphologies. Theses three factors show the most distinct localization of scenarios based on an energy evaluation for an entire year. Each factor has two values (define the scenarios) and three possible realizations (define the actual values in the energy system). The PV-generation factor values are named high PV (hPV) and low PV (lPV), the heating technology ones are HP and CHP, and the building insulation ones are modern insulation (mInsu) and old insulation (oInsu). Each factor value defines different probabilities for the realizations. Furthermore, a single realization is assumed as dominating, increasing its probability. For example, the value hPV has three realizations: The dominating realisation *high PV* (20-30 PV modules) has a probability of 50 %, *medium PV* (20-30 PV modules) has 25 %, and *no PV* has 25 %. These realizations yield 6.8 kW_p to 10.0 kW_p, 3.4 kW_p to 6.8 kW_p, and 0 kW_p, respectively. Both other factors, heating technology and building insulation, are also assigned with different probabilities for each realization. The heating factor defines the type of technology, which is implemented: *CHP*, *HP*, or no *electrical heating (non-el.)*. The insulation factor determines I_{spez}. For *passive*, $I_{\text{spez}} = 15\,\text{kWh/(m}^2\,\text{a)}$, for *modern* $I_{\text{spez}} = 50\,\text{kWh/(m}^2\,\text{a)}$, and for *old* $I_{\text{spez}} = 150\,\text{kWh/(m}^2\,\text{a)}$.

Figure 4 shows the scenarios, factors, and according probabilities of each realisation.

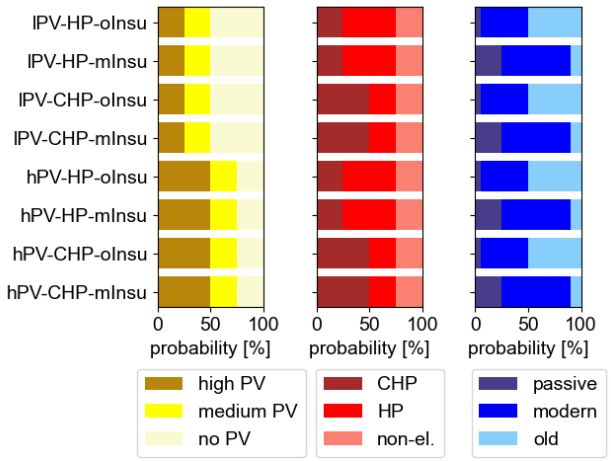

FIGURE 4. Scenarios, investigated by Monte-Carlo simulations; the permutations of high PV or low PV-generation, CHP or HP dominated, and modern or old insulation are shown. The length of a single bar-element shows the respective probability. Therefore, each bar sums to one. In total, eight scenarios are investigated.

B. SCENARIO-INDEPENDENT RANDOM FACTORS

The scenario-independent random factors are: Household structure, BEV probability, alignment of a PV system, and home energy storage (HES) availability.

The distribution of the household structure is modelled following statistical data for Germany. Singles without children, couples without children, singles with children, and couples with children household structures are considered. Their share in the overall system is derived from census data [41]. Furthermore, household types are divided into subtypes. Households with children are divided into one and two children households. According to data from [42], 67 % of singles with children have one child and 26 % have two childes and for couples, 53 % and 39 % have one child and two children, respectively. In addition, the employment status is taken into account. For singles with children, an employment rate of 75.5 % is assigned. For couples, the employment rate is 79.85 % [43]. 40.3 % of couples with children households have only one person being employed. Households without children are modelled with an employment rate of 92 % [44]. Due to demographics, a certain part of the households are modelled as retired. The retirement rate is set to 19 % [45]. The assumptions for household modelling are: Only one person of a household can be unemployed, the maximum number of children is two, and no children live in households with the retired employments status in order to reduce the model complexity and emphasize the major demographical structures.

Table 1 shows the distribution of households.

Battery electric vehicles (BEV) are considered to contribute to carbon dioxide reduction targets in the future, especially if electricity is generated with low carbon intensity [46]. However, there are other visions for future mobility provision, such as shifting away from car dependence towards public transport, cycling, or walking [47]. To account for this uncertainty, the probability of adding a BEV is set to 66 %. If a BEV is used, the technical parameters are gained from currently available models of different size.

TABLE 1. Demographics for the Monte-Carlo simulation. Four general types are modelled: Singles without children, couple without children, singles with children, and couple with children. The general types are further disaggregated to sub-types and the share of the sub-type on the overall populations is given. These shares are considered as probabilities in the Monte-Carlo simulation.

Household type/subtype	Share [%]
Singles without children	39.1
... retired	9.7
... working	27.3
... unemployed	2.1
Couples without children	26.5
... retired	7.2
... working	18.0
... one working	1.4
Singles with children	7.6
... working, 1 child	4.4
... working, 2 children	1.7
... unemployed, 1 child	1.4
... unemployed, 2 children	0.6
Couples with children	21.5
... working, 1 child	8.6
... working, 2 children	7.0
... one working, 1 child	5.8
... one working, 2 children	4.7

A further random parameter is PV-alignment. This parameter comprises the azimuth and inclination of the system. The azimuth has three distinct values, west, east, and south. Primarily, southern azimuth PV systems are built due to higher energy yield over the year [48], thus the souther azimuth is allocated with a probability of 80 % and the others with 10 %. The inclination is modelled by a normal distribution ($\mu = 30, \sigma = 5$).

Another random parameter models if a PV-system is combined with a HES system. In Germany, 50 % of recently build systems combine a PV with an HES system. Additionally, dropping prices of HES will increase the economic feasibility [49]. Therefore, the probability of combining a PV-system with a HES is increased and set to 75 %.

V. TIME SERIES AND COMPONENT MODELLING

This section describes the time series modelling and component dimensioning.

A. TIME SERIES MODELLING

For this study, electrical load, domestic hot water demand (DHW), BEV schedule for each vehicle, space heating, and PV generation time series are required.

1) ELECTRICAL LOAD AND DOMESTIC HOT WATER

The electrical load and DHW time series are calculated using the *Load Profile Generator (LPG)* [50]. This software tool

calculates the respective time series based on desires of household inhabitants. These desires are subsequently triggered to start an activity, where each activity is associated with a load profile. Using predefined household types, the LPG requires the household structure to be given, which describes the profession status and age of each member.

2) BEV SCHEDULE

The BEV schedules are modelled to be in line with the activities that shape the electrical load time series. This way, situations, such as arriving home and starting a washing machine afterwards, are considered. For BEV schedule modelling, the sequence of triggered activities from the LPG is extracted for each household member. Each activity is categorized as either a mobility demanding or a non-mobility demanding activity. Further, mobility demanding activities are categorized into three main purposes: Shopping, work, and spare time. For these three main purposes, distributions are fitted to model the trip length, according to *Mobilität in Deutschland* (MID) data [51], which is a nationwide transport behaviour survey of German households. It was found that the purpose work is most accurately approximated by a Burr distribution ($c = 1.36$, $d = 1.71$, location $= 0.01$, scale $= 19.7$), whereas shopping and holiday are approximated by a generalized inverse Gaussian distribution ($p = -1.53$, $b = 0.29$, location $= -0.58$, scale $= 37.3$ and $p = -0.94$, $b = 0.18$, location $= -0.67$, scale $= 60.2$, respectively). For this study, all distributions and the respective sampling are implemented using the SciPy package [52], therefore for parameter description follows the SciPy documentation.

For the shopping and spare time purposes, a new distance is drawn for each time the respective activity is triggered. The distance from the household to the working place usually stays constant. Therefore, the work purpose distance of each household member is drawn once for all trips in the schedule. Departure and return times are determined from the activation time of a mobility demanding activity and its consecutive one, respectively. The departure time is set equal to the triggering time of the mobility demanding activity and the triggering time of the subsequent one defines the return time. In Figure 5, the process for creating a single schedule is shown.

Furthermore, interdependencies of BEV usage between household members are considered. For each household, the number of available cars is determined by drawing a sample that describes the number of cars available, considering MID data [51]. The availability of a car for each person is determined, considering that only adults are allowed to use a car. If this is not the case, the individual schedules are merged. If two trips overlap during merging, one of the trips is discarded randomly, assuming that the discarded trip is not made with an electric car, but with another means of transport.

3) SPACE HEATING

The space heating (SH) demand is based on the floor area, insulation, and outdoor temperature. The floor area is drawn

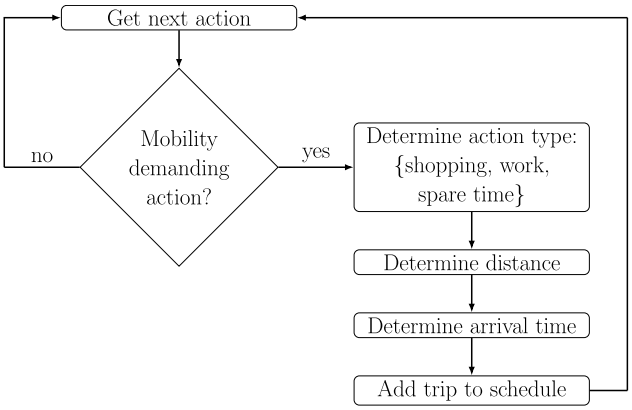

FIGURE 5. Flowchart of modelling a single BEV-schedule.

from distributions fitted to data from [41]. These distributions are fitted for: Singles, singles with children, couples, and couples with children. The areas for singles and singles with children are sampled from an exponentially modified Gaussian distribution ($K = -2.25$, location $= 59.2$, scale $= 13.7$ and $K = -1.64$, location $= 42.5$, scale $= 15.8$, respectively), couples from a reciprocal inverse Gaussian ($\mu = -0.059$, location $= -37.4$, scale $= 7.32$), and couples with children from a Jhonson SB ($a = -0.089$, $b = 1.44$, location $= 7.92$, scale $= 199$). The insulation is determined by the realized scenario. Data from Oldenburg, Germany, [53] is used for the outdoor temperature. The annual heat demand is calculated as:

$$E_a^{\mathrm{SH}} = I_{\mathrm{spez}} \cdot A_{\mathrm{house\ hold}} \cdot 1\,\mathrm{a} \tag{10}$$

The annual heat demand is distributed over the entire year using the *Degree-Day-Method* [54]. If the daily mean temperature $\theta_{\mathrm{ref},d}$ is lower than the reference temperature $\theta_{\mathrm{threshold}}(I_{\mathrm{spez}})$, the respective day requires heating. Building inertia is accounted for by considering the temperatures of previous days. $\theta_{\mathrm{threshold}}(I_{\mathrm{spez}})$ is calculated by linear interpolation, modelling the dependency on the household insulation I_{spez} [54]. The reference temperature for each day d is calculated as:

$$\theta_{\mathrm{ref},d} = \frac{\theta_d + \cdot 0.5 \cdot \theta_{d-1} + 0.25 \cdot \theta_{d-2} + 0.125 \cdot \theta_{d-3}}{1 + 0.5 + 0.25 + 0.125} \tag{11}$$

The degree day n_{HDD} is calculated according to:

$$n_{\mathrm{HDD},d} = \begin{cases} \theta_{\mathrm{ref},d} & \text{if } \theta_{\mathrm{ref}d} < \theta_{\mathrm{threshold}}(I_{\mathrm{spez}}) \\ 0 & \text{otherwise} \end{cases} \tag{12}$$

The space heating demand of each day is calculated as:

$$E_d^{\mathrm{SH}} = E_a^{\mathrm{SH}} \cdot \frac{n_{\mathrm{HDD},d}}{\sum_d n_{\mathrm{HDD},d}} \tag{13}$$

The procedure is repeated on the intra-day time scale to get the space heating demand for each minute, where the temperature inertia terms in Equation 11 are omitted.

4) PV TIME SERIES

The PV generation is modelled according to the same weather data as used for the space heating time series. For modelling, the software tool *pvlib* [55] is used. Each PV time series is based on the same module type and inverter. The inverter can convert up to 10 kW_p. Further parameters, i.e. the number modules, the system azimuth, and the system inclination, are extracted from the realized scenario.

B. COMPONENT DIMENSIONING

The components of an energy systems are dimensioned with respect to household specific requirements. For this study, detached houses, which accommodate a single household are the system boundary for dimensioning the heating system and HES. For each system, only discrete values are allowed, which reduces calculation complexity and reflects limited availability of system sizes in the real world market.

1) HES

The HES capacity dimensioning is based on [56]. Their methodology describes a technical approach of sizing a grid connected PV-battery system based on the degree of self-sufficiency (DSS). In this study the PV-size is determined by the scenario, thus, the only variable parameter is the HES capacity. The HES capacities are $\mathcal{C}_{\text{HES}} = \{0\,\text{kWh}, 0.5\,\text{kWh}, \ldots, 12\,\text{kWh}\}$ and the DSS for each capacity is calculated according to:

$$\text{DSS}_i(C^{\text{HES}}) = \frac{E^{\text{load}} - E^{\text{grid+}}(C^{\text{HES}})}{E^{\text{load}}} \quad \forall C^{\text{HES}} \in \mathcal{C}_{\text{HES}} \tag{14}$$

where E^{load} is the energy demand and $E^{\text{grid+}}(C^{\text{HES}})$ the energy from the grid, considering a certain capacity of the HES. The capacity at which the DSS is closes to target value $\text{DSS}_{\text{target}}$ is selected. For this study, $\text{DSS}_{\text{target}}$ is set to 75 % because higher values would result in rapid decrease of profitability [57]. Mathematically, this procedure is described as:

$$C^{\text{HES}}_{\text{selected}} = \arg\min_{C^{\text{HES}}} |\text{DSS}(C^{\text{HES}}) - \text{DSS}_{\text{target}}| \tag{15}$$

The power of a HES is calculated considering the medium power to capacity ratio is gained from [58]:

$$P^{\text{HES}}(C^{\text{HES}}_{\text{selected}}) = C^{\text{HES}}_{\text{selected}} \cdot 0.63\,\frac{\text{kW}}{\text{kWh}} \tag{16}$$

Furthermore, if a household consists of a BEV or a HP, the HES has usually higher capacities [59]. Therefore, if a household consists of a BEV, C^{HES} is increased by 3 kWh and if it consists of a HP, C^{HES} is increased by 1 kWh, according to [59]. The efficiency is drawn from a log-gamma distribution ($c = 0.93$, location $= 0.96$, scale $= 0.014$), where the parameters are fitted according to battery efficiencies from [58].

2) HEATING SYSTEM

The heating system is characterized by the thermal power of the generator P^{th} and the volume of the domestic heat storage V^{sys}. These values are determined by the *summation line method* [60]. That method requires the cumulative heating demand time series. For a given day d and minute m, the cumulative heating demand curve is calculated as

$$E_d^{\text{heat-c}}(m) = \sum_{i=1}^{m} E_{i,d}^{\text{SH}} + \sum_{i=1}^{m} E_{i,d}^{\text{DHW}}, \tag{17}$$

where each minutes i hot water demand and space heating demand is denoted by $E_{i,d}^{\text{DHW}}$ and $E_{i,d}^{\text{SH}}$, respectively. The sum is taken over the first m minutes of the day d.

The thermal power is dimensioned according to an optimization that searches for the minimum thermal power that is required to supply the cumulative heating demand. That procedure is individually performed for each day d as:

$$\min\ P_d^{\text{th}} \tag{18a}$$

$$\text{subject to } P_d^{\text{th}} \sum_{i=1}^{m} \Delta t_i - E_d^{\text{heat-c}}(m) \geq 0 \quad \forall m \tag{18b}$$

where $P_d^{\text{th}} \in \{500\,\text{W}, 1000\,\text{W}, \ldots\}$.

The energy storage capacity is required to cover the maximum distance between heat generation and demand curve of each day. However, the maximum distance often occurs in the later portions of the day that features low domestic hot water demand. In that case, the storage only absorbs excess generation. Therefore, smaller storage capacities can also be used if a control mechanism for the heating device is implemented. A sequence of operating states that describe either the state on or off, $s = (s_1, \ldots, s_M)$ with $s_m \in \{0, 1\}$ is defined to control the heating device for the M intervals. Therefore, the distance between the demand and generation curve is calculated as:

$$E_d^{\text{sys}} = \max_m \left(P_d^{\text{th}} \Delta t \sum_{i=1}^{m} s_i - E_d^{\text{heat-c}}(m) \right), \tag{19}$$

and the storage capacity for a day d is calculated according to:

$$\min\ E_d^{\text{sys}} \tag{20a}$$

$$\text{subjected to } P^{\text{th}} \Delta t \sum_{i=1}^{m} s_i - E_d^{\text{heat-c}}(m) \geq 0 \quad \exists s \forall m. \tag{20b}$$

We round E_d^{sys} to the next 0.1 kWh.

The required storage energy defines the volume of the storage according to:

$$V_d^{\text{sys}} = \frac{E_d^{\text{sys}}}{\rho_{H_2O} \cdot cp_{H_2O} \cdot \left(\theta_{\text{min}}^{\text{sys}} - \theta^{\text{DHW}}\right)}, \tag{21}$$

Finally, the design thermal power and storage volume are selected according to their maximum values over

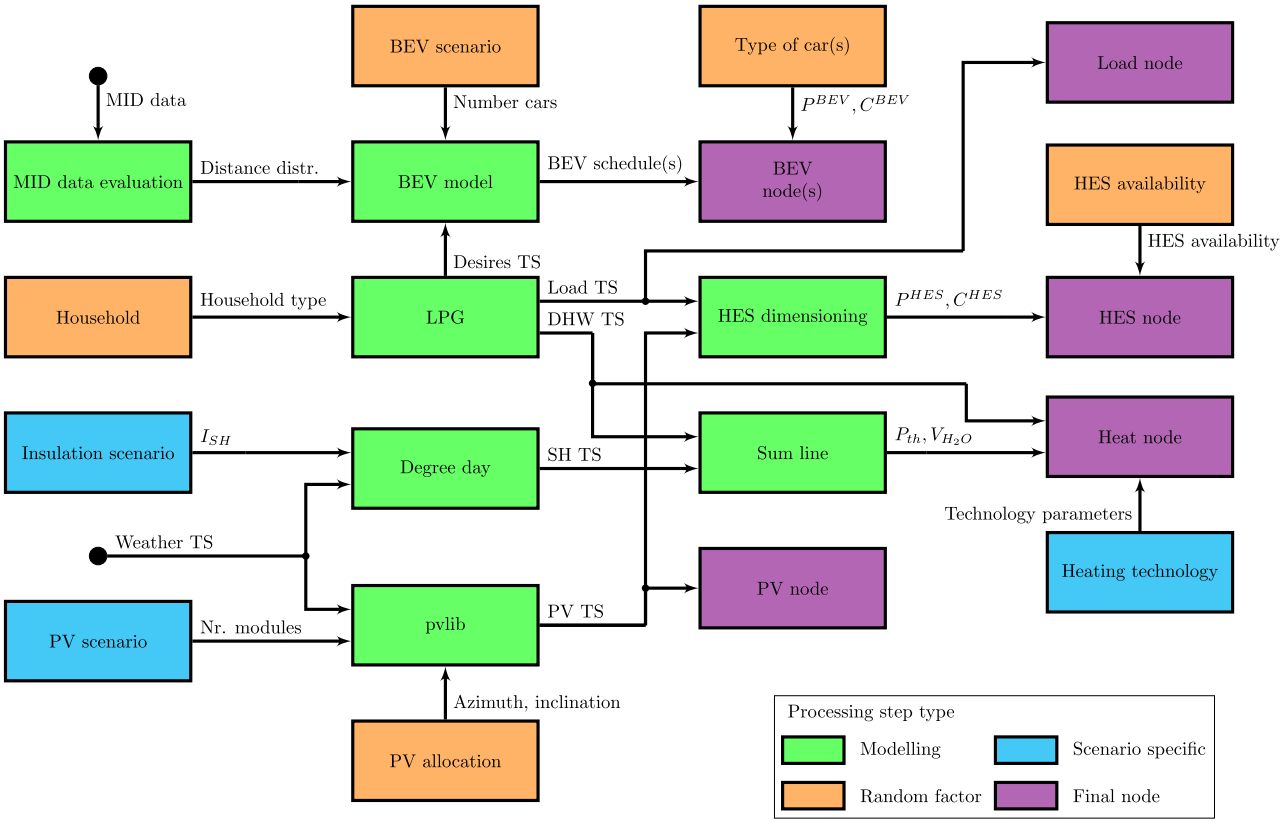

FIGURE 6. Dependencies on implemented technologies of a single house on the scenario, random factors, data, and models. Green boxes refer to models or data processing steps. Blue boxes show scenario specific steps. Orange boxes indicate random steps, in which a parameter is drawn on the same distribution for each scenario. The purple boxes describe the final node compilation.

all days:

$$P^{\text{th}} = \max_d(P_d^{\text{th}}) \tag{22}$$

$$V^{\text{sys}} = \max_d(V_d^{\text{sys}}) \tag{23}$$

In [13], a review on micro-CHP systems is presented. Established technologies, like Diesel powered CHP, range from 9 - 30 kW. However, hydrogen-based CHP systems are rather small. They are commercialized up to 5 kW. This respective maximum system size also results in the lowest operational cost [61]. For this study, if a hydrogen-based CHP system requires more than 5 kW of thermal power, an electrical BAK heating device is added to cope the additional thermal power.

VI. SIMULATION SET-UP

This section describes the links between scenarios, time series, and component dimensioning to configure a household. Moreover, the topology of the simulations, which describes a small district, the parameterization of the energy management algorithm, and the principle of the reference, which is used for comparison, are described.

A. MODEL LINKING

For this study, each device is represented by its own node. The energy management algorithm is based on multiple nodes that are orchestrated by auctioneers. The reference control scheme considers the devices independently of each other. Therefore, a node centric modelling enables simple calculation as all relevant data is condensed in the nodes attributes.

Weather data and the results of the LPG are the base for each household configuration.

The household electrical load is modelled by the LPG and used as the basis for the load node. The electrical load node is a part for each household.

The BEV model, described in Section V-A2, is used to define the BEV schedules. The BEV-scenario determines how many of these are included in the simulation in order to account for transport mode shift. According to Section IV-B, an EV is added with a probability of 66 %, otherwise it is assumed that public transport or other transport modes are used. Technical parameters, i.e. the maximum charging power P^{BEV} and capacity C^{BEV}, are determined randomly from a list of currently available BEVs.

The PV-system is modelled independently of the other nodes. From the scenario, the number of modules is

determined, which directly affects the maximum power of the PV-system. Azimuth and inclination are drawn randomly and serve as input parameters for *pvlib*, which returns the PV power time series.

PV systems can be combined with a HES to further match the electricity production and demand. The capacity C^{HES} and the maximum charging/discharging power $P^{\mathrm{HES}}(C^{\mathrm{HES}}_{\mathrm{selected}})$ of the respective HES are determines with the model described Section V-B1. The availability of an HES is determined randomly, preventing an HES to be added to each PV-system.

With the sum-line model from Section V-B2, the required thermal power P_{th} and storage volume V_{H_2O} of the heating system are modelled. The type of heating system implemented is determined with respect to the scenario. Figure 6 shows the required data and models for each step. These calculations are performed for each household individually and six configured household shape the energy systems under consideration.

B. TOPOLOGY AND ALGORITHM PARAMETER

The simulations are carried out for a small district size energy system. Each district consists of six households; each household is dimensioned according to Section VI-A. Therefore, each household consists of one to six devices. For the Monte-Carlo simulation, 400 different districts are modelled applying the algorithm and the reference control scheme to each of them.

As described in Section III-A, the algorithm coordinates the devices by means of auctioneers. For this study, the household connection auctioneers are configured to limit the summed power of the household between −14 kW and 14 kW. If the power lies within these limits, the auctioneer aggregates and forwards the indicated power of its children. If the power lies outside of these limits, the steering signal is adapted. The district auctioneer is set as a buffer auctioneer according to [38]. It is configured to achieve a residual power of 0 kW. However, if the load is low (< 5 kW) at high steering signals (80 % of $\mathrm{pr}_{\mathrm{max}}$), the auction is terminated. This allows to charge EVs at low power if no other significant loads are present and preserves HES capacity for times of high demand.

The reference control represents a status-quo approach. Each house is considered individually, thus the power of the district is the summed power of the connected houses. The devices are controlled as follows: Each heating device implements a hysteresis control, which uses the minimum storage temperature to activate the device and the maximum storage temperature to switch it off. The BEVs charge immediately with maximum possible power as they arrive at a respective house, and the HESs balance the power at the respective grid point. Balancing means, if excess power is generated by the devices of an household and the connected HES is not fully charged, the HES charges with the residual power, limited with its maximum power. In case of a power deficit, the HES operates vice versa.

Algorithm 1 Monte-Carlo Simulation

```
Select scenario under investigation
for j in [1, ..., 400] do
    for i in [1, ..., 6] do
        Draw scenario specific parameters according to Section IV - A
        Draw scenario independent parameters according to Section IV - B
        Generate household H_i according to FIGURE 6
    end for
    Combine households H_1 to H_6 to district D_j according to FIGURE 7
    Run the algorithm and reference for district D_j
    Calculate the KPIs K_j from the results of the algorithm and reference
end for
Evaluate the distributions for each KPI K for the algorithm and reference
```

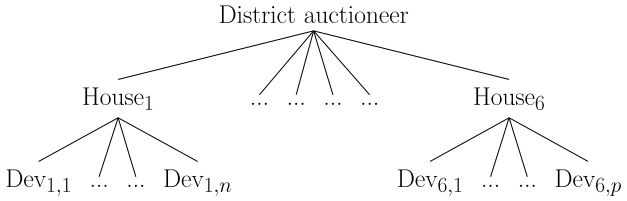

FIGURE 7. Topology of the energy system for the Monte-Carlo simulations.

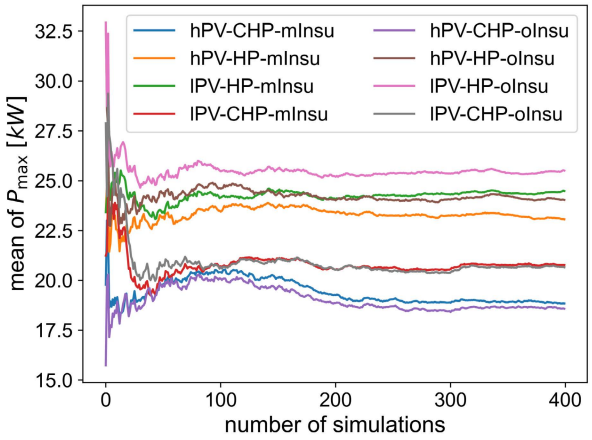

FIGURE 8. Convergence of the maximal power for the eight scenarios applying the algorithm.

The SOCs and storage temperatures at the beginning of the simulations are treated as uniformly distributed random variables that lie between the respective minimum and maximum value to avoid starting conditions which artificially trigger all devices to consume power, thus causing high peak loads.

C. MONTE-CARLO SIMULATION

Algorithm 1 describes the Monte-Carlo simulation procedure in pseudocode. It combines the elements from Section III

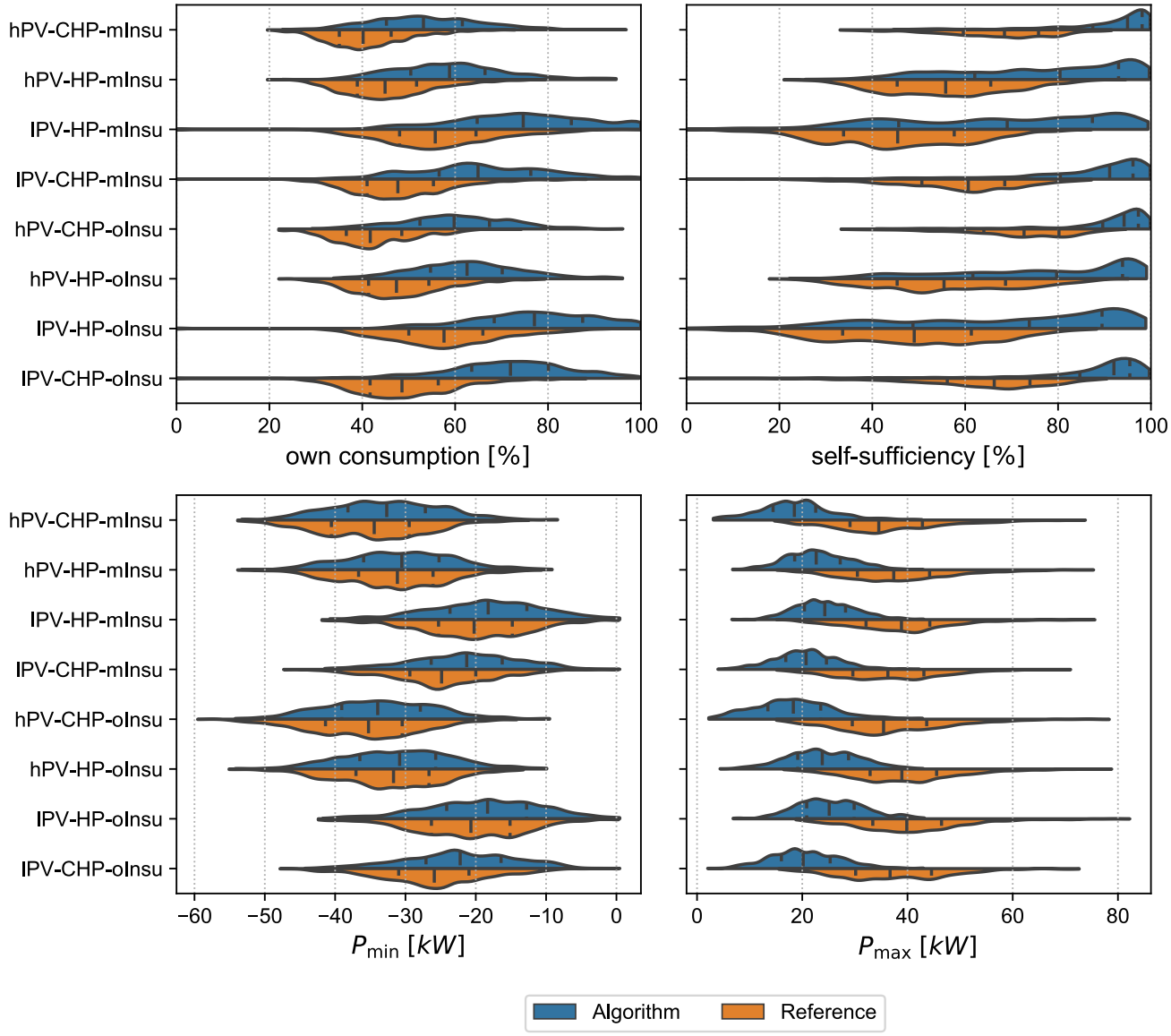

FIGURE 9. Violin plot of: Own consumption, self-sufficiency, min. power, and max. power distributions of the algorithm and reference for the different scenarios. The algorithms results are shown in blue at the top half for each curve and the references ones in orange at the bottom half for each scenario. The first, second and third quartile is tagged a dashed line.

to Section VI. These section cover dimensioning as well as operation, therefore the complexity can hardly be expressed in a single equation. The inherent complexity furthermore motivated the application of Monte-Carlo simulation.

VII. RESULTS

This section describes the convergence of the Monte-Carlo simulation and the results in terms of own-consumption, self-sufficiency, peak power, minimal power, energy exported and imported, the total energy produced by the CHP systems, and the energy discharged by the HESs.

1) CONVERGENCE

The Monte-Carlo method is a common tool to quantify uncertainty, however its application requires the assessment of its convergence [31]. Therefore, Figure 8 shows the mean of the peak power, calculated from an increasing number of simulations for each scenario. If the number of simulations is low, a single run heavily affects the mean. Therefore, big variations can be observed if the number of simulations is lower than 50. The simulation runs per scenarios are set to 400. At this number, no significant variations of the mean are observed. Furthermore, it keeps the computational effort manageable.

2) BASIC KPIs

In Figure 9 and 11, the results from the algorithm and the reference are compared with respect to the eight different scenarios. These figures are violin plots, displaying the statistical characteristics: 1st quartile, median, and 3rd quartile as well as the overall distribution by a kernel density estimation. Furthermore, Table 2 describes the differences of the algorithms and references medians for each scenario.

Figure 9 displays the four key performance indicators: Own consumption, self-sufficiency, minimal, and maximal (peak) power.

The algorithm increases the median own consumption, compared to the reference. As two percentages are compared, percentage points (p.p.) describe the difference between two values. The minimal increase is achieved for the hPV-CHP-mInsu scenario, where the algorithms median own consumption is 13.0 p.p. higher than the references one. For the lPV-CHP-oInsu scenario, the difference showed the highest value, i.e. 23.4 p.p. That scenario has the highest share of flexible generation, due to the combination of CHP with poor insulation and low PV generation. Therefore, the flexibility of the CHP can be utilized by the algorithm. The scenarios with the lowest increase in own consumption are a combination of modern building insulation and high PV generation. It demonstrates that the high generation limits the potential of the advanced energy management algorithm because the flexibility requirement is reduced.

Self-sufficiency is also increased across the scenarios. The median is 21.5 p.p. to 30.4 p.p. greater for the algorithm, compared to the reference. The biggest increase is achieved in the lPV-CHP-mInsu scenario. As for own consumption, the biggest advantage of the algorithm occurred in scenarios that consist of low inflexible generation shares. The modern building insulation fosters the algorithms advantage over the reference. A reduced heating demand results in lower CHP utilization. The algorithm tailors the reduced generation to the demand, thus archiving a bigger advantage over the uncoordinated reference approach. Note the degree of self sufficiency is still higher for scenarios that combine CHP with poor building insulation due to the higher heating demand as can be seen in the top right panel of Figure 9. In general, the algorithm achieves high values of self-sufficiency across all the scenarios, as indicated by the high probability mass that lies within 90 % to 100 %.

For minimal power, the differences between both control approaches are small. The proposed algorithm achieved a higher median (closer to zero) across the scenarios, but only in the range of 0.6 kW to 3.7 kW. This can be explained by the effect of the inflexible PV generation. Peak generation occurs in summer around noon. At this time, heat demand is usually low and EVs are not available, as they are used for getting to work. However, there is an improvement gained by the algorithm because is can decrease the fed in power from CHP systems in times of high PV generation. That effect is shown by the slightly reduced feed-in power. For CHP dominated scenarios, the difference range from 1.3 kW to 3.7 kW, whereas HP dominated ones range from 0.6 kW to 2.4 kW.

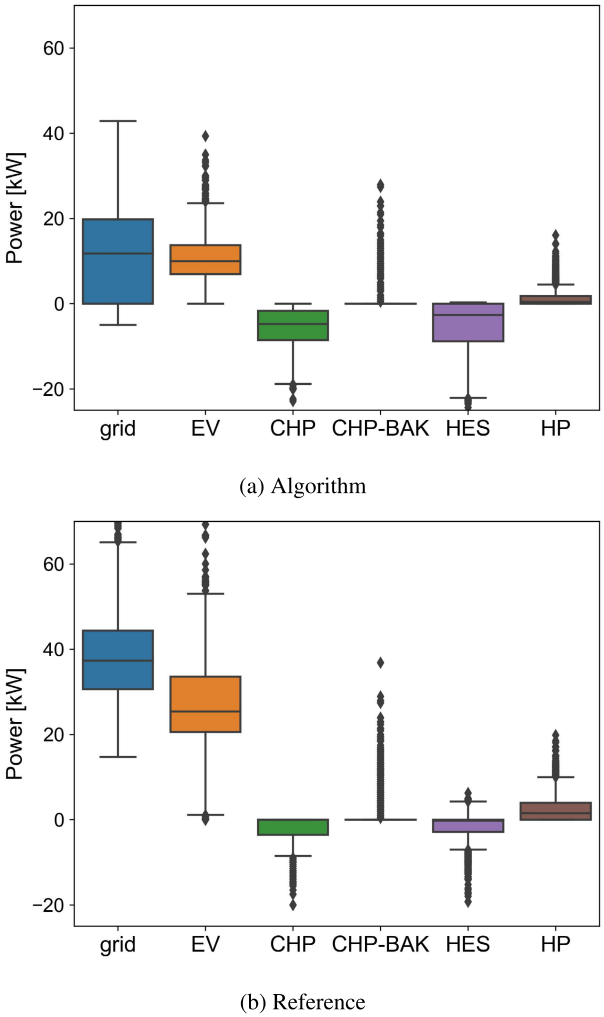

(a) Algorithm

(b) Reference

FIGURE 10. Box plot of the summed power for the grid connection, EV, CHP, HES, and HP during reference peak load times. Household and PV values are identical at each investigated time interval and, therefore not shown. The results are gained from all scenarios.

The algorithm reduces the median peak loads by 15 kW to 17 kW. Although the median for all the scenarios are similar, the biggest reduction was achieved by CHP dominated scenarios, indicating that the algorithm utilizes the CHP systems to mitigate peak loads.

To further investigate the peak load differences, the powers for each component at peak load times is shown in Figure 10. Figure 10a displays the algorithms results and Figure 10b the references ones. The comparison shows that different components contribute to reduce the algorithms peak loads. The biggest difference lies in EVs power distribution. This agrees with literature, which identifies EVs as a major power demand factor [62]. The median and extreme values are around 20 kW bigger for the reference. Furthermore, the heat pump electricity consumption is lower for the algorithm, as indicated by the smaller box. Besides the load side, higher

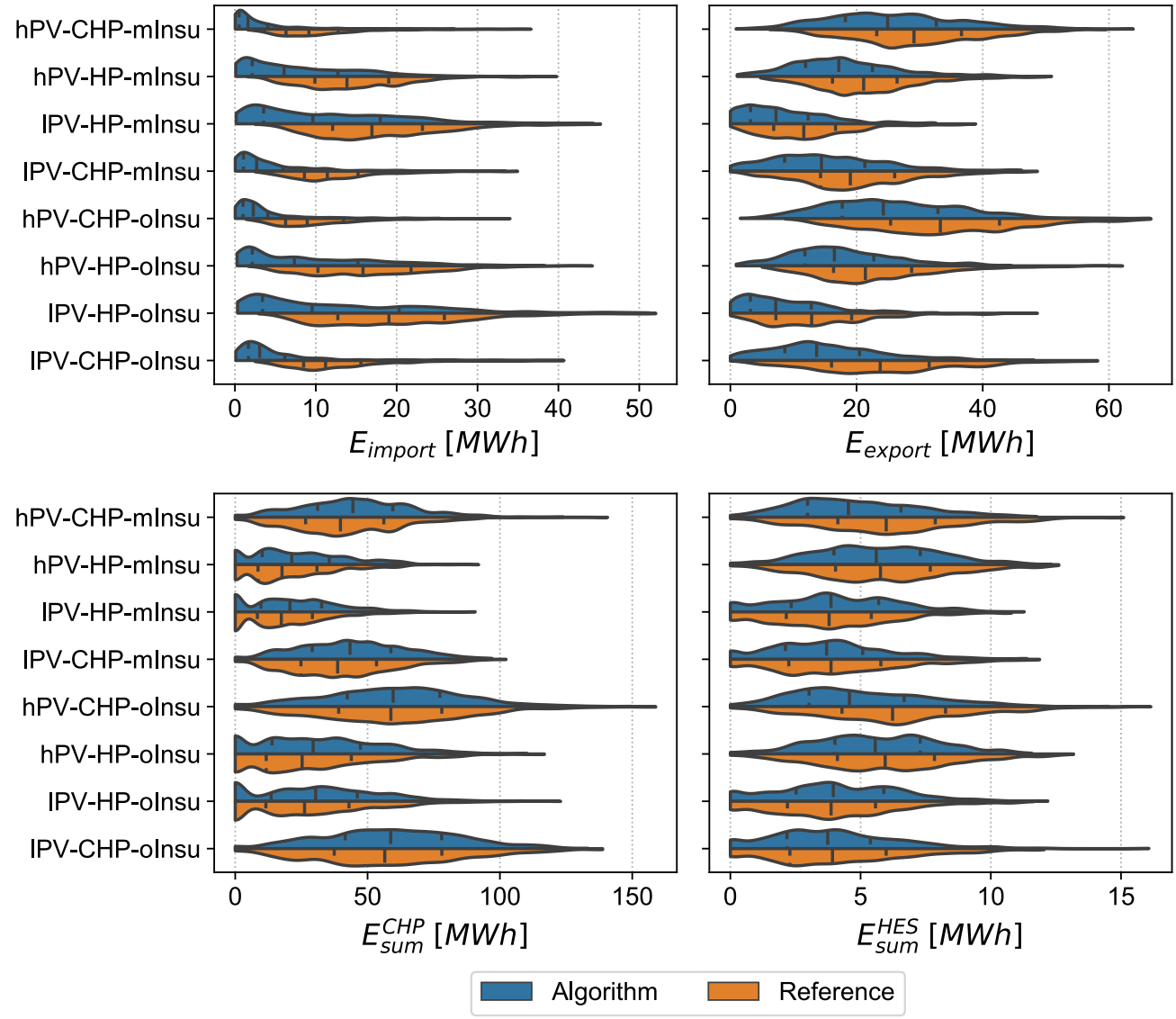

FIGURE 11. Energy results for different scenarios. The amount of energy (heating plus electrical) is calculated for the entire duration of a single simulation (1 year). As for Figure 9, the first, second and third quartile is tagged a dashed line. Note the energy from the CHP system does not consider the energy produced by the backup and the HES energy only considers the discharged energy.

generation also mitigates peak load. This is shown by bigger boxes for CHP generation and the box for the HES is further located in the discharge region.

3) ENERGY EVALUATION

Figure 11 displays the distributions of exported and imported electrical energy, the energy produced by the CHP systems as well as the discharged energy of the HESs. It shows that the improvements in self-sufficiency and own consumption are achieved by reducing export and import. A significant proportion of the imported energy probability mass lies between 0 MWh to 10 MWh. Therefore, energy export is overall higher than import, as more probability mass lies at higher values for energy export. Furthermore, the energy from CHP in the bottom panel of Figure 11 indicates the advantage of improved building insulation. The scenarios which combine CHP with old building insulation, hPV-CHP-oInsu and lPV-CHP-oInsu, result in higher energy produced by the CHP systems. This reflects the high space heating demand in these scenarios. The HP dominated scenarios show multimodal distributions and for each of them one maximum lies at 0 MWh. These maxima are caused be scenario realisations that do not implement CHP systems, which is much more likely for the HP dominated scenarios than for the CHP ones. Additionally, it shows the independent generation profiles of the CHP and PV system, as the PV scenario has a minor effect on the CHP energy production.

The simulations for the algorithm and the reference are based on identical heat demand; in theory, leading to equal overall energy production for the CHP. However, the backup

TABLE 2. Differences between the median of the algorithm and reference for the KPIs. They are calculated as: $KPI_{algorithm} - KPI_{reference}$. Note that a positive difference for min. power means that the respective value is closer to 0kW as the minimum power is lower than 0kW in each scenario. The difference between two percentage values is given in percentage points (p.p.).

Scenario	Difference to reference			
	Own consumption	Self-sufficiency	Min. power	Max. power
hPV-CHP-mInsu	+ 13.0 p.p.	+ 26.5 p.p.	+ 1.8 kW	- 16.0 kW
hPV-HP-mInsu	+ 13.9 p.p.	+ 24.6 p.p.	+ 0,6 kW	- 14,7 kW
lPV-HP-mInsu	+ 18.9 p.p.	+ 23.6 p.p.	+ 2,0 kW	- 14,6 kW
lPV-CHP-mInsu	+ 17.3 p.p.	+ 30.4 p.p.	+ 3,6 kW	- 15,5 kW
hPV-CHP-oInsu	+ 18.1 p.p.	+ 21.5 p.p.	+ 1,3 kW	- 17,2 kW
hPV-HP-oInsu	+ 15.2 p.p.	+ 24.2 p.p.	+ 0,9 kW	- 15,1 kW
lPV-HP-oInsu	+ 19.5 p.p.	+ 24.8 p.p.	+ 2,4 kW	- 14,7 kW
lPV-CHP-oInsu	+ 23.4 p.p.	+ 25.8 p.p.	+ 3,7 kW	- 16,5 kW

systems are not considered. The difference between the distributions for the algorithm and the reference is caused by varying utilization of the backup systems. The algorithm makes scarcer use of the backup system and, therefore, increases the total energy produced by the CHP system.

The algorithm reduces the discharged energy for scenarios that are characterized by a higher share of CHP systems, especially if combined with high share of bigger PV systems. Additional, for HP scenarios, the available PV power determines the HES utilization. If high HP shares are combined with the high PV scenario, the algorithm discharges slightly more energy from the HESs, whereas for low PV scenarios the reference utilize the HESs to a higher degree.

VIII. DISCUSSION AND CONCLUSION

The proposed Monte-Carlo simulation has the advantage that the results are distributions. This makes the results more robust compared to a single case study, as a wider range of system configurations is explored. The results can be used for grid planning and allow an integrated view of sector-coupled energy systems. In the conventional planning and simulation process, predefined time series serve as a basis [63]. In this study, however, synthetic time series, based on demographic data, and scenarios are used. Furthermore, the proposed simulation methodology is based on the behaviour of individual persons, which is why it is not necessary to resort to simultaneity factors. These simultaneity factors are frequently used means of grid dimensioning [64].

From the different scenarios, it is shown that intelligent energy management provides varying benefit. The algorithm achieves the greatest advantage over the reference for scenarios with low inflexible generation. For low PV scenarios, the algorithm achieves an own consumption that is 17.3 p.p. to 23.4 p.p. higher than the result from the reference, whereas the high PV scenarios result in a difference of 13.0 p.p. to 18.1 p.p. This difference demonstrates the improved utilization of scarce local electricity by the algorithm.

A big advantage of the algorithm is peak load reduction. This is primary achieved by controlled charging of the BEVs. Other contributing factors are higher fed in power by the CHPs and HESs as well as lower power operation of the HPs.

Furthermore, the selection of KPIs plays a crucial role in evaluating the scenarios. This is shown as scenarios with poor building insulations result in higher own consumption. However, the CHPs generate more energy, which results in higher fuel demand for the respective districts.

The results are a basis for decision-making in order to evaluate the advantages of intelligent energy management. Specifically, this paper compares an algorithm based on coordination with a reference that does not require coordination. If the reduced peak load avoids grid expansion, cost are saved which can compensate the additional communication hardware expense. Uncertainty, for example due to varying EV integration, is taken into account by the proposed method, performing a risk assessment. In addition, the scenario-based evaluation can compare different technology concepts with each other. Here, it can be weighed up what the effects of higher PV output, heat pumps instead of CHP systems, or the share of EVs in the system is.

The scenario space and probabilities of the technologies are based on assumption that are derived form [40]. Varying the probabilities alter the results as they determine the occurrence of a technology in this Monte-Carlo approach. They play an important role if the edges of the distributions are the focus of investigation. The results can be interpreted as a general trend of the influence of a technology if all but one scenario factor remains constant. Furthermore, additional technologies, for instance district heating systems, can be integrated to cover a bigger scenario space.

The weather time series in this work only represents one region. Variations could arise due to different

weather patterns. For example, PV systems are more effective in the southern German regions than in the North. This spatial effect is not covered in this study as the location is not part of the scenario space.

Furthermore, the technology choices consider single independent households. Systems that are connected to a district heating system with a single big generation unit for all households or apartment buildings are not modelled. However, the algorithm shows distinct advantages over the reference in terms of reduced peak load. Reducing these loads is especially interesting for weak electricity grids. These grids are often found in rural regions where detached single family houses are build, motivating the parameter selection for this study.

Another factor of uncertainty is demographics. This study is based on German average data for the household distribution. The residential structures can exhibit a bigger degree of homogeneity, e.g. due to high shares of people with similar personal living condition.

At last, sociological characteristics, for example a preference for renewable electricity, are not considered. These could be integrated into the demand and supply function in order to model them and increase the flexibility of the overall system.

The methodology of this study can be applied to different use cases as the algorithms under consideration can be freely exchanged. For this study, the methodology serves to compare an energy management algorithm to a reference that represents an uncoordinated system. The same physical component models are used for the algorithm and the reference. Only the control functions for these components vary. In some cases, algorithms model components with a varying level of detail, for instance linear vs. non-linear. This has to be considered if the methodology is applied to other energy management approaches.

REFERENCES

[1] G. Luderer, R. C. Pietzcker, S. Carrara, H. S. de Boer, S. Fujimori, N. Johnson, S. Mima, and D. Arent, "Assessment of wind and solar power in global low-carbon energy scenarios: An introduction," *Energy Econ.*, vol. 64, pp. 542–551, May 2017.

[2] B. V. Mathiesen, H. Lund, D. Connolly, H. Wenzel, P. A. Østergaard, B. Möller, S. Nielsen, O. Ridjan, P. Karnøe, K. Sperling, and F. K. Hvelplund, "Smart energy systems for coherent 100% renewable energy and transport solutions," *Appl. Energy*, vol. 145, pp. 139–154, May 2015.

[3] W. Zappa, M. Junginger, and M. van den Broek, "Is a 100% renewable European power system feasible by 2050?" *Appl. Energy*, vols. 233–234, pp. 1027–1050, Jan. 2019.

[4] M. Robinius, A. Otto, P. Heuser, L. Welder, K. Syranidis, D. Ryberg, T. Grube, P. Markewitz, R. Peters, and D. Stolten, "Linking the power and transport sectors—Part 1: The principle of sector coupling," *Energies*, vol. 10, no. 7, p. 956, Jul. 2017.

[5] A. Jambagi, M. Kramer, and V. Cheng, "Electricity and heat sector coupling for domestic energy systems—Benefits of integrated energy system modelling," in *Proc. 4th Int. Conf. Smart Cities Green ICT Syst.*, 2015, pp. 1–6.

[6] K. Witkowski, P. Haering, S. Seidelt, and N. Pini, "Role of thermal technologies for enhancing flexibility in multi-energy systems through sector coupling: Technical suitability and expected developments," *IET Energy Syst. Integr.*, vol. 2, no. 2, pp. 69–79, Jun. 2020.

[7] J. Love, A. Z. P. Smith, S. Watson, E. Oikonomou, A. Summerfield, C. Gleeson, P. Biddulph, L. F. Chiu, J. Wingfield, C. Martin, A. Stone, and R. Lowe, "The addition of heat pump electricity load profiles to GB electricity demand: Evidence from a heat pump field trial," *Appl. Energy*, vol. 204, pp. 332–342, Oct. 2017.

[8] D. Fischer and H. Madani, "On heat pumps in smart grids: A review," *Renew. Sustain. Energy Rev.*, vol. 70, pp. 342–357, Oct. 2017.

[9] E. Merkel, R. McKenna, and W. Fichtner, "Optimisation of the capacity and the dispatch of decentralised micro-CHP systems: A case study for the U.K.," *Appl. Energy*, vol. 140, pp. 120–134, Feb. 2015.

[10] P. E. Dodds, I. Staffell, A. D. Hawkes, F. Li, P. Grünewald, W. McDowall, and P. Ekins, "Hydrogen and fuel cell technologies for heating: A review," *Int. J. Hydrogen Energy*, vol. 40, no. 5, pp. 2065–2083, 2015.

[11] Y. Ligen, H. Vrubel, and H. Girault, "Mobility from renewable electricity: Infrastructure comparison for battery and hydrogen fuel cell vehicles," *World Electr. Vehicle J.*, vol. 9, no. 1, p. 3, May 2018.

[12] O. Gröger, H. A. Gasteiger, and J.-P. Suchsland, "Review—Electromobility: Batteries or fuel cells?" *J. Electrochem. Soc.*, vol. 162, no. 14, pp. A2605–A2622, 2015.

[13] S. Martinez, G. Michaux, P. Salagnac, and J.-L. Bouvier, "Micro-combined heat and power systems (micro-CHP) based on renewable energy sources," *Energy Convers. Manage.*, vol. 154, pp. 262–285, Dec. 2017.

[14] Y. Manoharan, S. E. Hosseini, B. Butler, H. Alzhahrani, B. T. F. Senior, T. Ashuri, and J. Krohn, "Hydrogen fuel cell vehicles; current status and future prospect," *Appl. Sci.*, vol. 9, no. 11, p. 2296, Jun. 2019.

[15] U. Salahuddin, H. Ejaz, and N. Iqbal, "Grid to wheel energy efficiency analysis of battery- and fuel cell-powered vehicles," *Int. J. Energy Res.*, vol. 42, no. 5, pp. 2021–2028, Apr. 2018.

[16] E. Ucer, M. C. Kisacikoglu, and A. C. Gurbuz, "Learning EV integration impact on a low voltage distribution grid," in *Proc. IEEE Power Energy Soc. Gen. Meeting (PESGM)*, Aug. 2018, pp. 1–5.

[17] T. Aziz and N. Ketjoy, "PV penetration limits in low voltage networks and voltage variations," *IEEE Access*, vol. 5, pp. 16784–16792, 2017.

[18] M. Jaxa-Rozen and E. Trutnevyte, "Sources of uncertainty in long-term global scenarios of solar photovoltaic technology," *Nature Climate Change*, vol. 11, no. 3, pp. 266–273, Mar. 2021.

[19] T. W. Brown, T. Bischof-Niemz, K. Blok, C. Breyer, H. Lund, and B. V. Mathiesen, "Response to 'Burden of proof: A comprehensive review of the feasibility of 100% renewable-electricity systems,'" *Renew. Sustain. Energy Rev.*, vol. 92, pp. 834–847, Sep. 2018.

[20] C. Rottondi, M. Duchon, D. Koss, A. Palamarciuc, A. Pití, G. Verticale, and B. Schätz, "An energy management service for the smart office," *Energies*, vol. 8, no. 10, pp. 11667–11684, Oct. 2015.

[21] N. G. Paterakis, O. Erdinç, A. G. Bakirtzis, and J. P. S. Catalão, "Optimal household appliances scheduling under day-ahead pricing and load-shaping demand response strategies," *IEEE Trans. Ind. Informat.*, vol. 11, no. 6, pp. 1509–1519, Dec. 2015.

[22] T. Taniguchi, K. Kawasaki, Y. Fukui, T. Takata, and S. Yano, "Automated linear function submission-based double auction as bottom-up real-time pricing in a regional Prosumers' electricity network," *Energies*, vol. 8, no. 7, pp. 7381–7406, Jul. 2015.

[23] W. El-Baz, P. Tzscheutschler, and U. Wagner, "Integration of energy markets in microgrids: A double-sided auction with device-oriented bidding strategies," *Appl. Energy*, vol. 241, pp. 625–639, May 2019.

[24] Y. Du and F. Li, "Intelligent multi-microgrid energy management based on deep neural network and model-free reinforcement learning," *IEEE Trans. Smart Grid*, vol. 11, no. 2, pp. 1066–1076, Mar. 2020.

[25] S. Haghifam, K. Zare, M. Abapour, G. Muñoz-Delgado, and J. Contreras, "A Stackelberg game-based approach for transactive energy management in smart distribution networks," *Energies*, vol. 13, no. 14, p. 3621, Jul. 2020.

[26] Y. Wang, W. Saad, Z. Han, H. V. Poor, and T. Basar, "A game-theoretic approach to energy trading in the smart grid," *IEEE Trans. Smart Grid*, vol. 5, no. 3, pp. 1439–1450, May 2014.

[27] M. A. Hossain, H. R. Pota, S. Squartini, and A. F. Abdou, "Modified PSO algorithm for real-time energy management in grid-connected microgrids," *Renew. Energy*, vol. 136, pp. 746–757, Jun. 2019.

[28] Y. Liu, Y. Li, H. B. Gooi, Y. Jian, H. Xin, X. Jiang, and J. Pan, "Distributed robust energy management of a multimicrogrid system in the real-time energy market," *IEEE Trans. Sustain. Energy*, vol. 10, no. 1, pp. 396–406, Jan. 2019.

[29] B. Anderson, S. Lin, A. Newing, A. Bahaj, and P. James, "Electricity consumption and household characteristics: Implications for census-taking in a smart metered future," *Comput., Environ. Urban Syst.*, vol. 63, pp. 58–67, May 2017.
[30] A. Kavousian, R. Rajagopal, and M. Fischer, "Ranking appliance energy efficiency in households: Utilizing smart meter data and energy efficiency frontiers to estimate and identify the determinants of appliance energy efficiency in residential buildings," *Energy Buildings*, vol. 99, pp. 220–230, Jul. 2015.
[31] F. Ballio and A. Guadagnini, "Convergence assessment of numerical Monte Carlo simulations in groundwater hydrology," *Water Resour. Res.*, vol. 40, no. 4, Apr. 2004, Art. no. W04603.
[32] R. G. McClarren, *Uncertainty Quantication and Predictive Computational Science*. Cham, Switzerland: Springer, 2018.
[33] Y. Xiang, J. Liu, and Y. Liu, "Robust energy management of microgrid with uncertain renewable generation and load," *IEEE Trans. Smart Grid*, vol. 7, no. 2, pp. 1034–1043, Mar. 2016.
[34] X. Lu, Z. Liu, L. Ma, L. Wang, K. Zhou, and N. Feng, "A robust optimization approach for optimal load dispatch of community energy hub," *Appl. Energy*, vol. 259, Feb. 2020, Art. no. 114195.
[35] Y. Iwafune, K. Ogimoto, Y. Kobayashi, and K. Murai, "Driving simulator for electric vehicles using the Markov chain Monte Carlo method and evaluation of the demand response effect in residential houses," *IEEE Access*, vol. 8, pp. 47654–47663, 2020.
[36] A. Jahid, M. S. Hossain, M. K. H. Monju, M. F. Rahman, and M. F. Hossain, "Techno-economic and energy efficiency analysis of optimal power supply solutions for green cellular base stations," *IEEE Access*, vol. 8, pp. 43776–43795, 2020.
[37] S. Senemar, M. Rastegar, M. Dabbaghjamanesh, and N. Hatziargyriou, "Dynamic structural sizing of residential energy hubs," *IEEE Trans. Sustain. Energy*, vol. 11, no. 3, pp. 1236–1246, Jul. 2020.
[38] S. Arens, S. Schlüters, B. Hanke, K. von Maydell, and C. Agert, "Multi-unit Japanese auction for device agnostic energy management," *Int. J. Electr. Power Energy Syst.*, vol. 136, Mar. 2022, Art. no. 107350.
[39] M. Nazari-Heris, S. Abapour, and B. Mohammadi-Ivatloo, "Optimal economic dispatch of FC-CHP based heat and power micro-grids," *Appl. Thermal Eng.*, vol. 114, pp. 756–769, Mar. 2017.
[40] S. Arens, S. Schlüters, B. Hanke, K. V. Maydell, and C. Agert, "Sustainable residential energy supply: A literature review-based morphological analysis," *Energies*, vol. 13, no. 2, p. 432, Jan. 2020.
[41] (2011). *Zensusdatenbank des Zensus 2011*. Accessed: Dec. 22, 2021. [Online]. Available: https://ergebnisse.zensus2011.de/
[42] (2019). *Familien Nach Zahl Der Minderjährigen Kinder*. Accessed: Dec. 22, 2021. [Online]. Available: https://www.destatis.de/DE/Themen/Gesellschaft-Umwelt/Bevoelkerung/Haus%halte-Familien/Tabellen/2-5-familien.html
[43] (2018). *Alleinerziehende in Deutschland 2017*. Accessed: Dec. 22, 2021. [Online]. Available: https://www.destatis.de/DE/Presse/Pressekonferenzen/2018/Alleinerziehen%de/pressebroschuere-alleinerziehende.pdf
[44] V. Steiner, "The labor market for older workers in Germany," *J. Labour Market Res.*, vol. 50, no. 1, pp. 1–14, Aug. 2017.
[45] (2019). *Bevölkerung Im Wandel Annahmen Und Ergebnisse der 14. Koordinierten Bevölkerungsvorausberechnung*. Accessed: Dec. 22, 2021. [Online]. Available: https://www.destatis.de/DE/Presse/Pressekonferenzen/2019/Bevoelkerung/p%ressebroschuere-bevoelkerung.pdf
[46] A. M. Andwari, A. Pesiridis, S. Rajoo, R. Martinez-Botas, and V. Esfahanian, "A review of battery electric vehicle technology and readiness levels," *Renew. Sustain. Energy Rev.*, vol. 78, pp. 414–430, Oct. 2017.
[47] R. Buehler, J. Pucher, R. Gerike, and T. Götschi, "Reducing car dependence in the heart of Europe: Lessons from Germany, Austria, and Switzerland," *Transp. Rev.*, vol. 37, no. 1, pp. 4–28, Jan. 2017.
[48] S. Killinger, D. Lingfors, Y.-M. Saint-Drenan, P. Moraitis, W. van Sark, J. Taylor, N. A. Engerer, and J. M. Bright, "On the search for representative characteristics of PV systems: Data collection and analysis of PV system azimuth, tilt, capacity, yield and shading," *Sol. Energy*, vol. 173, pp. 1087–1106, Oct. 2018.
[49] K.-P. Kairies, J. Figgener, D. Haberschusz, O. Wessels, B. Tepe, and D. U. Sauer, "Market and technology development of PV home storage systems in Germany," *J. Energy Storage*, vol. 23, pp. 416–424, Jun. 2019.
[50] N. Pflugradt and B. Platzer, "Behavior based load profile generator for domestic hot water and electricity use," in *Proc. Int. Conf. Energy Storage (Innostock)*, Lleida, Spain, 2012.
[51] B. Lenz, C. Nobis, K. Köhler, M. Mehlin, R. Follmer, D. Gruschwitz, B. Jesske, and S. Quandt, "Mobilität in deutschland 2008," in *Infas—Institut Für Angewandte Sozialwissenschaft GmbH und Deutsches Zentrum Für Luft-Und Raumfahrt E.V. Institut Für Verkehrsforschung, Report*. Berlin, Germany: INFAS Institut für Angewandte Sozialwissenschaft GmbH; Deutsches Zentrum für Luft- und Raumfahrt e.V.Institut für Verkehrsforschung, 2010.
[52] P. Virtanen, R. Gommers, T. E. Oliphant, M. Haberland, T. Reddy, D. Cournapeau, E. Burovski, P. Peterson, W. Weckesser, J. Bright, and S. J. Van Der Walt, "SciPy 1.0: Fundamental algorithms for scientific computing in Python," *Nature Methods*, vol. 17, pp. 261–272, Feb. 2020.
[53] J. Kalisch, T. Schmidt, D. Heinemann, and E. Lorenz, "Continuous meteorological observations in high-resolution (1Hz) at University of Oldenburg (2014–08)," Carl-von-Ossietzky Univ. Oldenburg, Oldenburg, Germany, Tech. Rep., 2015. Accessed: Jan. 3, 2022. [Online]. Available: https://doi.pangaea.de/10.1594/PANGAEA.847830, doi: 10.1594/PANGAEA.847830.
[54] W. Heitkoetter, W. Medjroubi, T. Vogt, and C. Agert, "Regionalised heat demand and power-to-heat capacities in Germany—An open dataset for assessing renewable energy integration," *Appl. Energy*, vol. 259, Feb. 2020, Art. no. 114161.
[55] W. Holmgren, C. Hansen, and M. Mikofski, "Pvlib Python: A Python package for modeling solar energy systems," *J. Open Source Softw.*, vol. 3, no. 29, p. 884, 2018.
[56] B. Boeckl and T. Kienberger, "'Sizing of PV storage systems for different household types,'" *J. Energy Storage*, vol. 24, Aug. 2019, Art. no. 100763.
[57] V. Bertsch, J. Geldermann, and T. Lühn, "What drives the profitability of household PV investments, self-consumption and self-sufficiency?" *Appl. Energy*, vol. 204, pp. 1–15, Oct. 2017.
[58] J. Weniger, S. Maier, N. Orth, and V. Quaschning, "Stromspeicher-inspektion 2020," HTW Berlin, Berlin, Germany, Tech. Rep., 2020. Accessed: Jan. 3, 2022. [Online]. Available: https://pvspeicher.htw-berlin.de/wp-content/uploads/Stromspeicher-Inspektion-2020.pdf
[59] J. Figgener, P. Stenzel, K.-P. Kairies, J. Linßen, D. Haberschusz, O. Wessels, G. Angenendt, M. Robinius, D. Stolten, and D. U. Sauer, "The development of stationary battery storage systems in Germany—A market review," *J. Energy Storage*, vol. 29, Jun. 2020, Art. no. 101153.
[60] C. Ihle, R. Bader, and M. Golla, *Tabellenbuch Sanitär Heizung Lüftung Klima/Lüftung*, vol. 7. Cologne, Germany: Bildungsverlag EINS, 2008.
[61] D. Yu, Y. Meng, G. Yan, G. Mu, D. Li, and S. L. Blond, "Sizing combined heat and power units and domestic building energy cost optimisation," *Energies*, vol. 10, no. 6, p. 771, Jun. 2017.
[62] G. Benetti, D. Caprino, M. L. D. Vedova, and T. Facchinetti, "Electric load management approaches for peak load reduction: A systematic literature review and state of the art," *Sustain. Cities Soc.*, vol. 20, pp. 124–141, Jan. 2016.
[63] E. Hartvigsson, J. Ehnberg, E. O. Ahlgren, and S. Molander, "Linking household and productive use of electricity with mini-grid dimensioning and operation," *Energy Sustain. Develop.*, vol. 60, pp. 82–89, Feb. 2021.
[64] L. P. Fernandez, T. G. S. Román, R. Cossent, C. M. Domingo, and P. Frias, "Assessment of the impact of plug-in electric vehicles on distribution networks," *IEEE Trans. Power Syst.*, vol. 26, no. 1, pp. 206–213, May 2011.

STEFAN ARENS received the B.Sc. degree in process engineering and energy technology from the Bremerhaven University of Applied Sciences, in 2014, and the M.Sc. degree in engineering physics with a specialization in renewable energy from Carl von Ossietzky Universität Oldenburg, Oldenburg, Germany, in 2018. He is currently pursuing the Ph.D. degree with the Energy Systems Technology Department, DLR Institute of Networked Energy Systems, Oldenburg. His research interests include smart energy management systems, energy forecasting, and application scenarios of energy management systems.

SUNKE SCHLÜTERS received the Ph.D. degree in pure mathematics from Carl von Ossietzky Universität Oldenburg, Germany, in 2015, and switched to the field of energy management research, in 2018. He is currently working as a Researcher and a Project Manager working on energy management strategies and algorithms with the DLR Institute of Networked Energy Systems. His research interest includes machine learning-based self-optimizing energy management systems.

BENEDIKT HANKE received the Ph.D. degree in engineering from the Albert-Ludwigs-Universität Freiburg im Breisgau, in 2010, researching the dielectric constant of polymer ceramic composites. He worked in the field of material research for silicon thin film photovoltaics for several years. He is currently a Team Leader at the DLR Institute of Networked Energy Systems heading the Energy Management Group. His research interests include low-maintenance, low-cost energy management systems based on machine learning approaches, as well as methods for minimal energy system design by optimization of operational strategies.

KARSTEN VON MAYDELL received the M.Sc. degree in physics from the University of Oldenburg, Germany, in 2000, and the Ph.D. degree in physics from the University of Marburg, Germany, in 2003. From 2000 to 2006, he worked as a Graduate Research Assistant, a Postdoctoral Researcher, and a Project Manager at the Helmholtz-Zentrum Berlin. From 2006 to 2007, he worked as a Project Manager Research and Development at Q-Cells AG Thalheim, Germany. From 2007 to 2008, he was a Group Leader at the Energy and Semiconductor Research Laboratory, University of Oldenburg. From 2008 to 2014, he was the Head of the Division Photovoltaic, NEXT ENERGY Research Institute, Oldenburg, Germany. Since 2017, he has been the Head of the Energy Systems Technology Department, DLR Institute of Networked Energy Systems. His research interests include the design of energy systems, smart energy management for grid connected and off-grid connected systems, integration of flexibilities in energy systems, and robust operation of power grids.

CARSTEN AGERT received the Ph.D. degree in physics, in 2001, based on his research work from the Fraunhofer Institute for Solar Energy Systems, Freiburg, Germany, and the University of Oxford, U.K. He studied physics at the University of Marburg, Germany, and the University of Canterbury, U.K. He was a Scholar of the Studienstiftung. In 2001, he worked as a Postdoctoral Researcher with Pretoria, South Africa. From 2002 to 2005, he was a Research Associate with the German Advisory Council on Global Change (WBGU). Subsequently, he was the Head of the Fuel Cell Systems Research Group, Fraunhofer Institute for Solar Energy Systems, from 2005 to 2008. Since 2008, he has been a Full Professor with the University of Oldenburg and the Director of the DLR Institute of Networked Energy Systems, until 2017 known as the NEXT ENERGY Institute. His research interests include materials and device development for energy converters, research into electrical energy technologies and systems, as well as energy systems analysis.